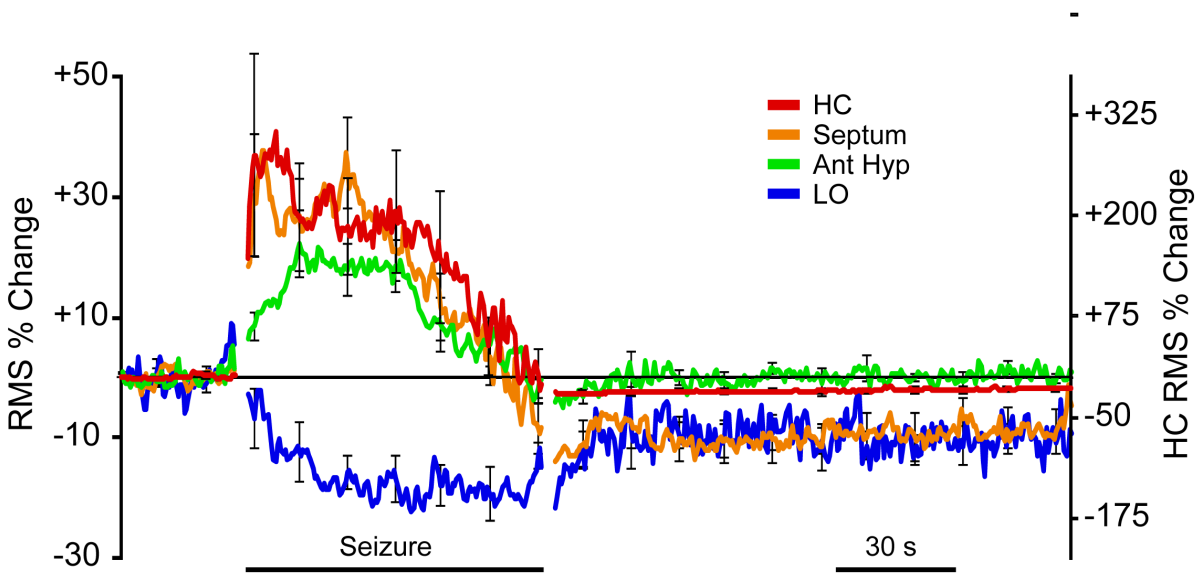
+50
+30
+10
-10
-30
RMS % Change
+325
+200
+75
-50
-175
HC RMS % Change
HC
Septum
Ant Hyp
LO
Seizure
30 s

Figure S1, Related to Figures 2 and 3

Multiunit activity matches BOLD changes.

(Left scale) The lateral septum (Septum) and anterior hypothalamus (Ant Hyp) show increased ictal multiunit activity (MUA), which decreases below baseline in the postictal period. The ictal activity matches BOLD changes while the postictal MUA decreases more quickly than the BOLD signal (**Figures 2, 3B, and 3C**). MUA in the lateral orbital frontal cortex (LO) is suppressed ictally and remains suppressed for duration of the displayed postictal period.

(Right scale) MUA in hippocampus (HC) is dramatically increased during the seizure and decreases back to baseline in the postictal period. Like the lateral septum and anterior hypothalamus, the BOLD increases are matched by MUA increases ictally but the MUA activity decreases postictally more quickly than the BOLD signal (**Figures 2, 3B and 3C**).

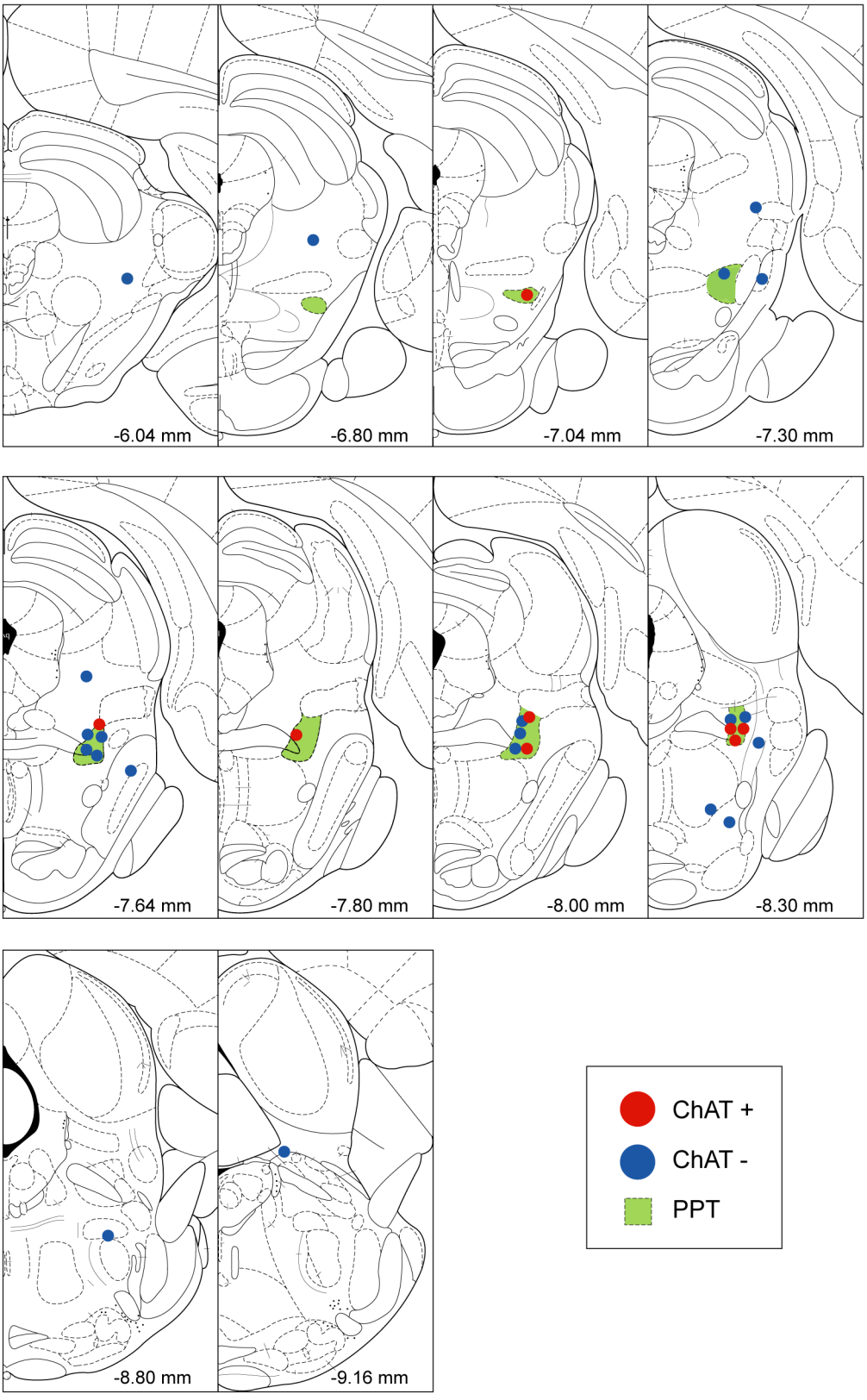
-6.04 mm
-6.80 mm
-7.04 mm
-7.30 mm
-7.64 mm
-7.80 mm
-8.00 mm
-8.30 mm
-8.80 mm
-9.16 mm
ChAT +
ChAT -
PPT

Figure S2, Related to Figures 4 and 6

Anatomical distribution of recovered cells in PPT.

Locations of pedunculopontine tegmental nucleus (PPT) and peri-PPT cells recovered during juxtacellular recordings. Cholinergic cells are distributed through the rostral-caudal axis of PPT, and non-cholinergic cells are located either in PPT or in the adjacent brainstem tegmentum. Cells co-staining for choline acetyltransferase are ChAT+. Cells not co-staining for choline acetyltransferase are ChAT-. AP coordinates are in millimeters relative to bregma. Schematics taken with permission from Paxinos and Watson (Paxinos and Watson, 1998).

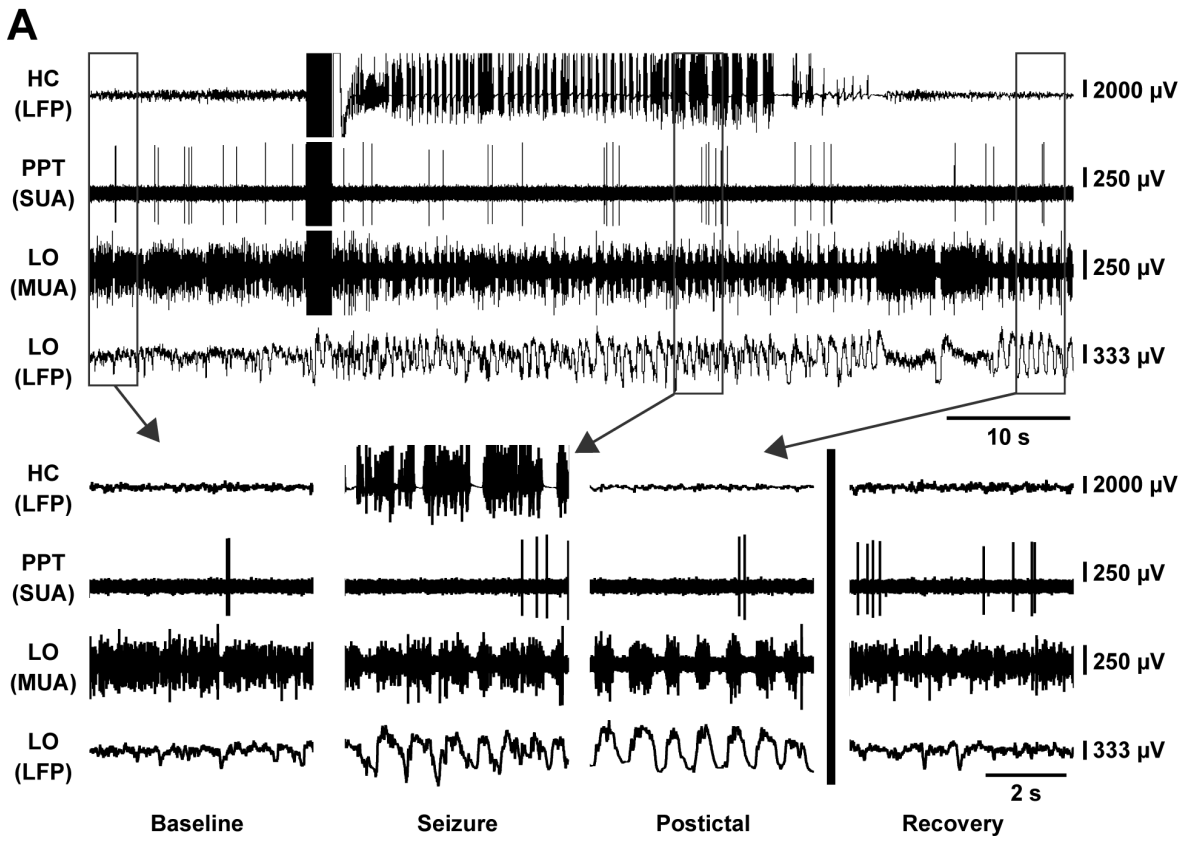
A
HC (LFP)
PPT (SUA)
LO (MUA)
LO (LFP)
2000 µV
250 µV
250 µV
333 µV
10 s
HC (LFP)
PPT (SUA)
LO (MUA)
LO (LFP)
2000 µV
250 µV
250 µV
333 µV
2 s
Baseline
Seizure
Postictal
Recovery

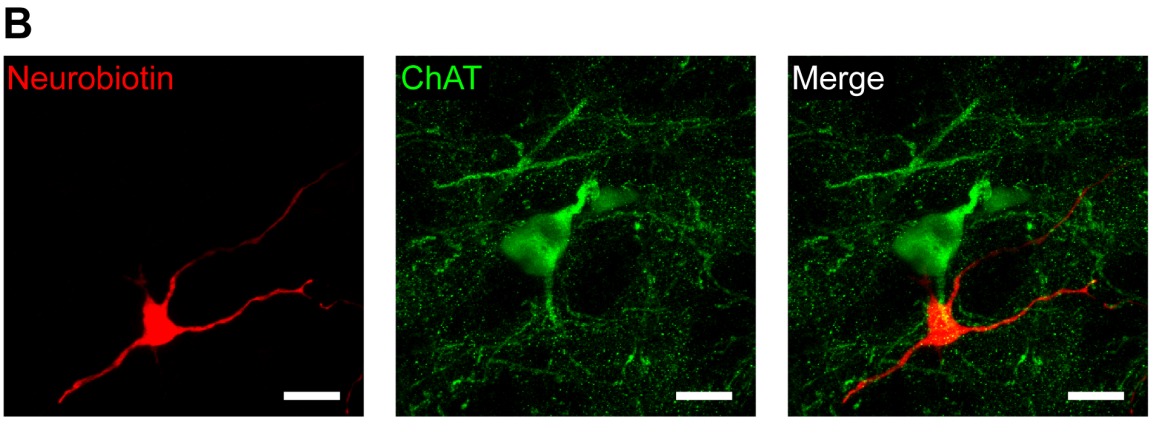
B
Neurobiotin
ChAT
Merge

Figure S3, Related to Figure 6

Non-cholinergic neuron in PPT does not change behavior during seizure activity.

(A) Example of a non-cholinergic neuron during a partial seizure. Expanded segments of baseline, seizure, and postictal recordings from the boxed regions in (A) as well as a recovery period 3 minutes after the stimulus.

(B) Labeled non-cholinergic cell recorded in (A), stained with Neurobiotin in left panel, choline acetyltransferase (ChAT) in middle panel, and merge in right panel. Scale bars are 20 micrometers. HC, hippocampus; PPT pedunculopontine tegmental nucleus; LO, lateral orbitofrontal cortex; LFP, local field potential; SUA, single unit (juxtacellular) activity; MUA, multiunit activity.

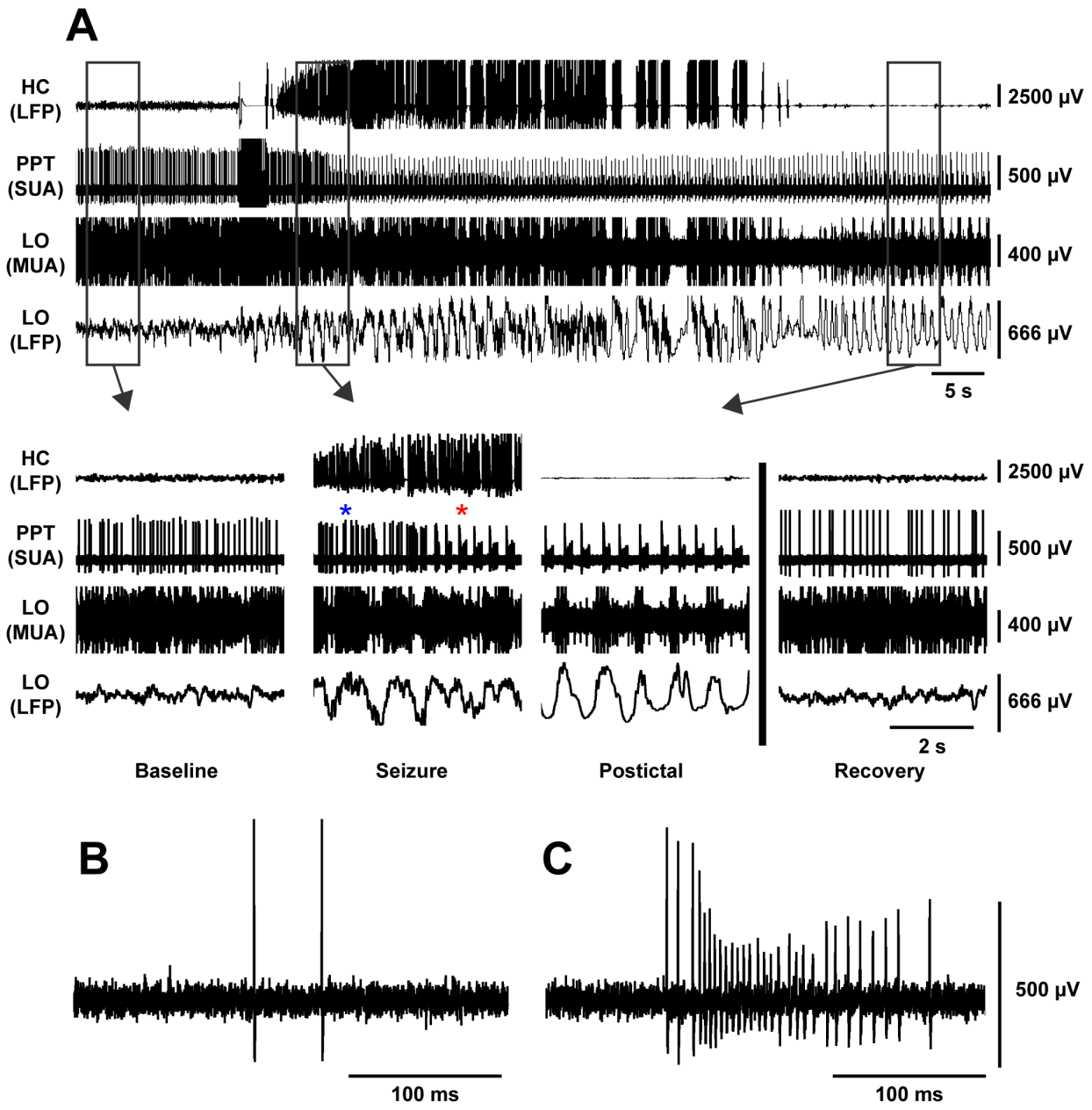
A
HC (LFP)
PPT (SUA)
LO (MUA)
LO (LFP)
2500 µV
500 µV
400 µV
666 µV
5 s
HC (LFP)
PPT (SUA)
LO (MUA)
LO (LFP)
2500 µV
500 µV
400 µV
666 µV
2 s
Baseline
Seizure
Postictal
Recovery
B
100 ms
C
500 µV
100 ms

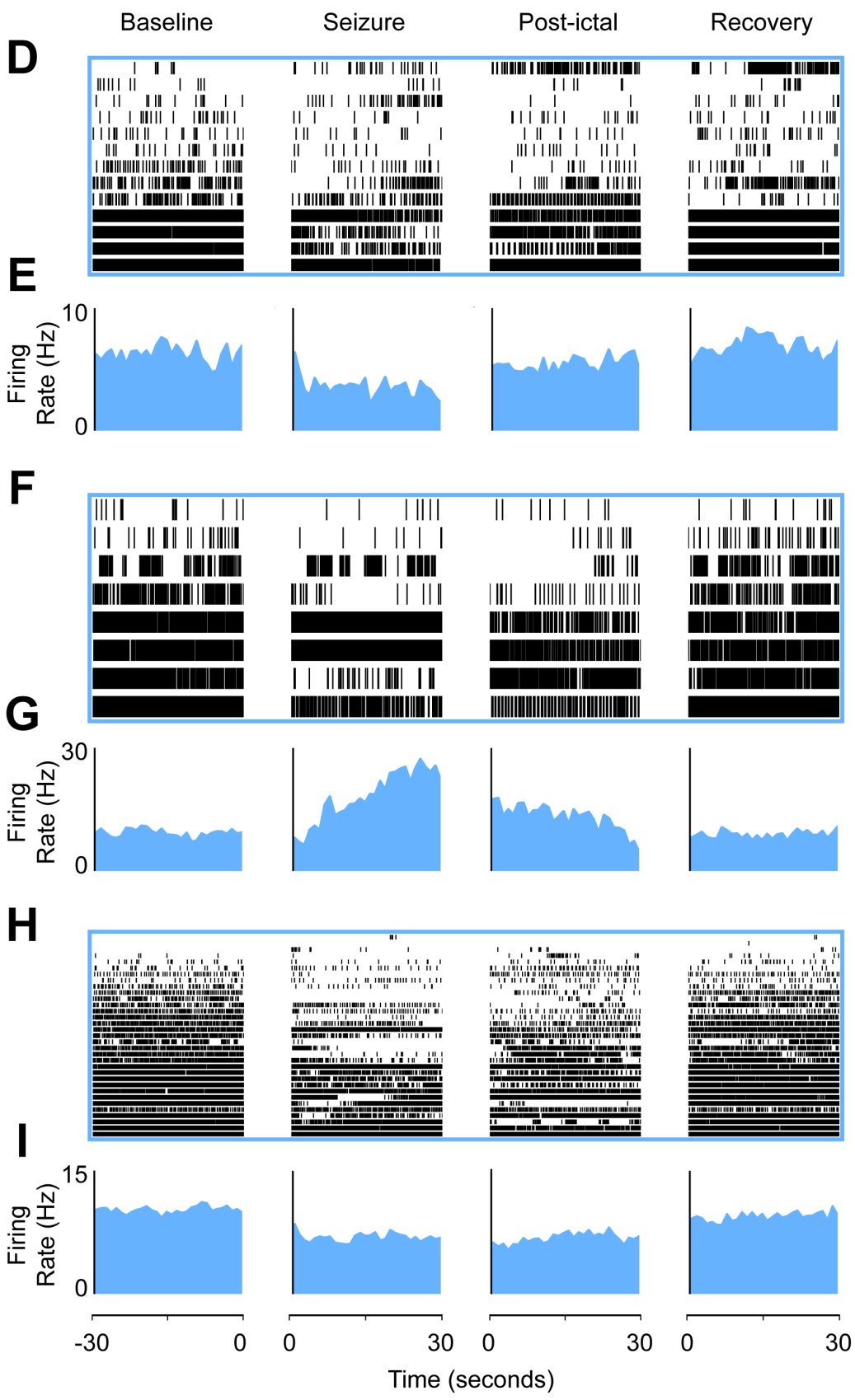
Baseline
Seizure
Post-ictal
Recovery
D
E
F
G
H
I
Firing Rate (Hz)
10
0
30
0
15
0
-30
0
0
30
0
30
0
30
Time (seconds)

Figure S4, Related to Figure 6

Some non-cholinergic neurons in the PPT region convert to burst-firing during partial seizures while unrecovered cells in the PPT region decreased overall firing during partial seizures.

(A) A recording from a partial seizure. Expanded segments of baseline, seizure, and postictal recordings from the boxed regions in (A) as well as a recovery period 6 minutes after the stimulus. At baseline the PPT neuron fired regularly. During the seizure, the neuron initially appeared unchanged but then converted from tonic firing to burst firing during the course of the seizure. The burst firing persisted postictally but returned to normal firing during recovery after the seizure.

(B) An enlarged time scale of the blue asterisk in (A, Seizure) during the initial phase of the seizure shows two, non-burst action potentials.

(C) An enlarged time scale of the red asterisk in (A, seizure) shows the neuron converted to burst firing.

(D) Raster plot shows the individual action potentials of the recovered, non-bursting, non-cholinergic neurons (13 cells from 13 animals) during the 30 seconds prior to seizure initiation (“Baseline”), first 30 seconds of the seizure (“Seizure”), first 30 seconds following seizure end (“Postictal”), and 30 seconds after the animal has returned to baseline (“Recovery”).

(E) Mean firing rates of recovered, non-bursting, non-cholinergic neurons in 1-second bins across Baseline, Seizure, Postictal, and Recovery periods. Non-bursting non-cholinergic neurons on average showed a trend towards reduced firing rate during seizures, which did not reach statistical significance. 13 cells; mean seizure duration

61.11 seconds ± 7.06 seconds; comparing seizure to baseline: mean change in firing rate -2.44 Hz ± 1.17 Hz; paired t-test, $P = 0.06$.

(F) Raster plot shows the individual action potentials of the recovered, bursting, non-cholinergic neurons (8 cells from 8 animals) during “Baseline,” “Seizure,” “Postictal,” and “Recovery.”

(G) Mean firing rates of recovered, bursting, non-cholinergic neurons in 1-second bins across Baseline, Seizure, Postictal, and Recovery periods. Bursting non-cholinergic neurons on average showed a trend towards increased firing rate during seizures, which did not reach statistical significance. 8 cells; mean seizure duration 63.93 seconds ± 9.00 seconds; comparing seizure to baseline: mean change in firing rate +6.71 Hz ± 8.84 Hz; paired t-test, $P = 0.47$.

(H) Raster plot of unrecovered cells (33 cells from 19 animals) reveals variable changes during seizure during “Baseline,” “Seizure,” “Postictal,” and “Recovery.”

(I) Mean firing rate histogram data of all non-recovered neurons. Mean firing rate significantly decreased during seizures. 33 neurons from 19 animals: mean seizure duration 54.73 seconds ± 6.22 seconds; comparing seizure to baseline: mean change in firing rate -3.44 Hz ± 0.72 Hz; paired t-test Holm-Bonferroni corrected, $P < 0.05$. HC, hippocampus; PPT pedunculopontine tegmental nucleus; LO, lateral orbitofrontal cortex; LFP, local field potential; SUA, single unit (juxtacellular) activity; MUA, multiunit activity. Neurons in raster plots (D, F, and H) are ordered based on baseline firing rate for visualization.

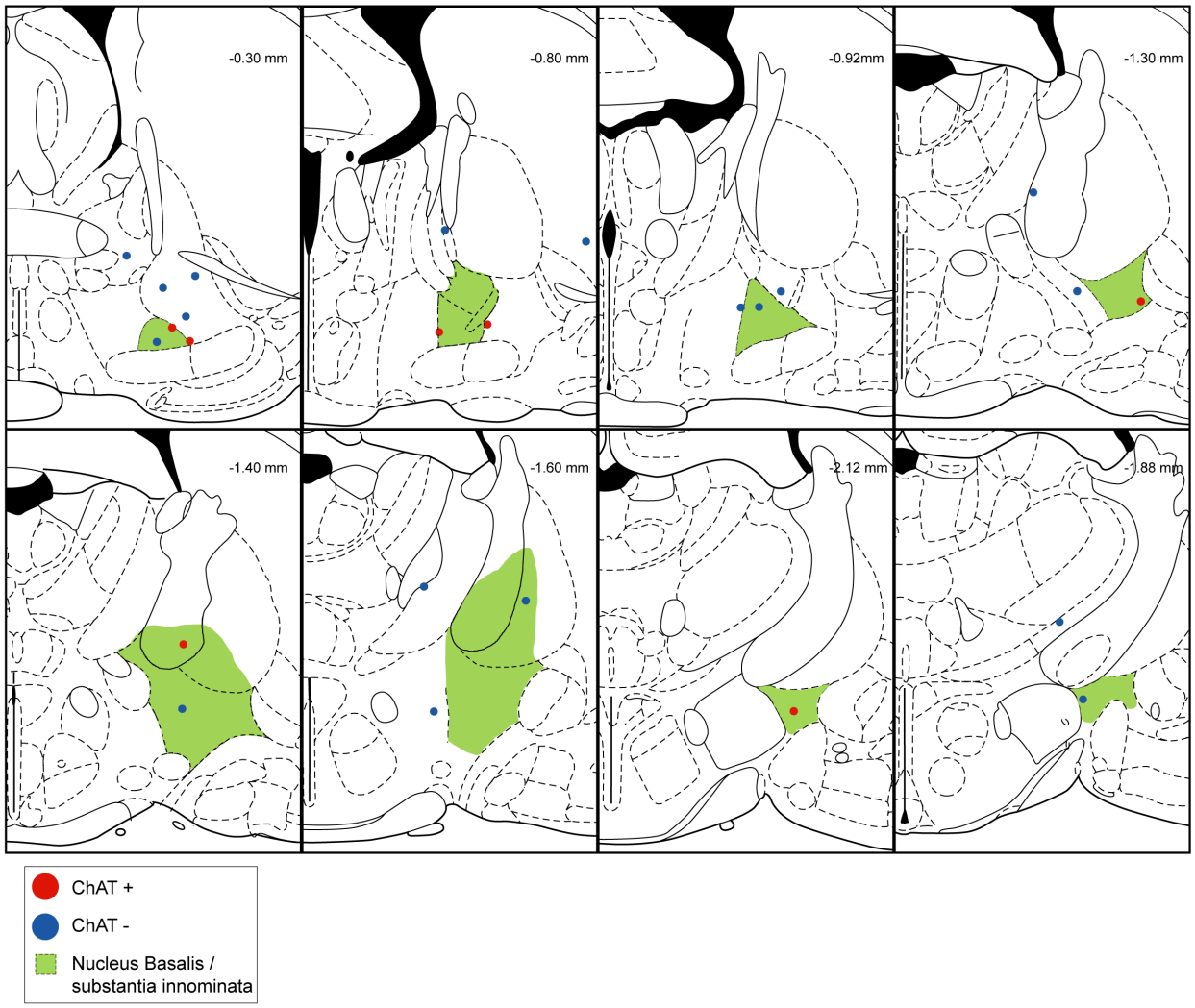
-0.30 mm
-0.80 mm
-0.92mm
-1.30 mm
-1.40 mm
-1.60 mm
-2.12 mm
-1.88 mm
ChAT +
ChAT -
Nucleus Basalis / substantia innominata

Figure S5, Related to Figures 5 and 6

Anatomical distribution of recovered cells in basal forebrain.

Locations of basal forebrain and peri-basal forebrain cells recovered during juxtacellular recordings. Cholinergic cells are distributed throughout the basal forebrain nuclei including nucleus basalis and substantia innominata. Cells co-staining for choline acetyltransferase are ChAT+. Cells not co-staining for choline acetyltransferase are ChAT-. AP coordinates are in millimeters relative to bregma. Schematics taken with permission from Paxinos and Watson (Paxinos and Watson, 1998).

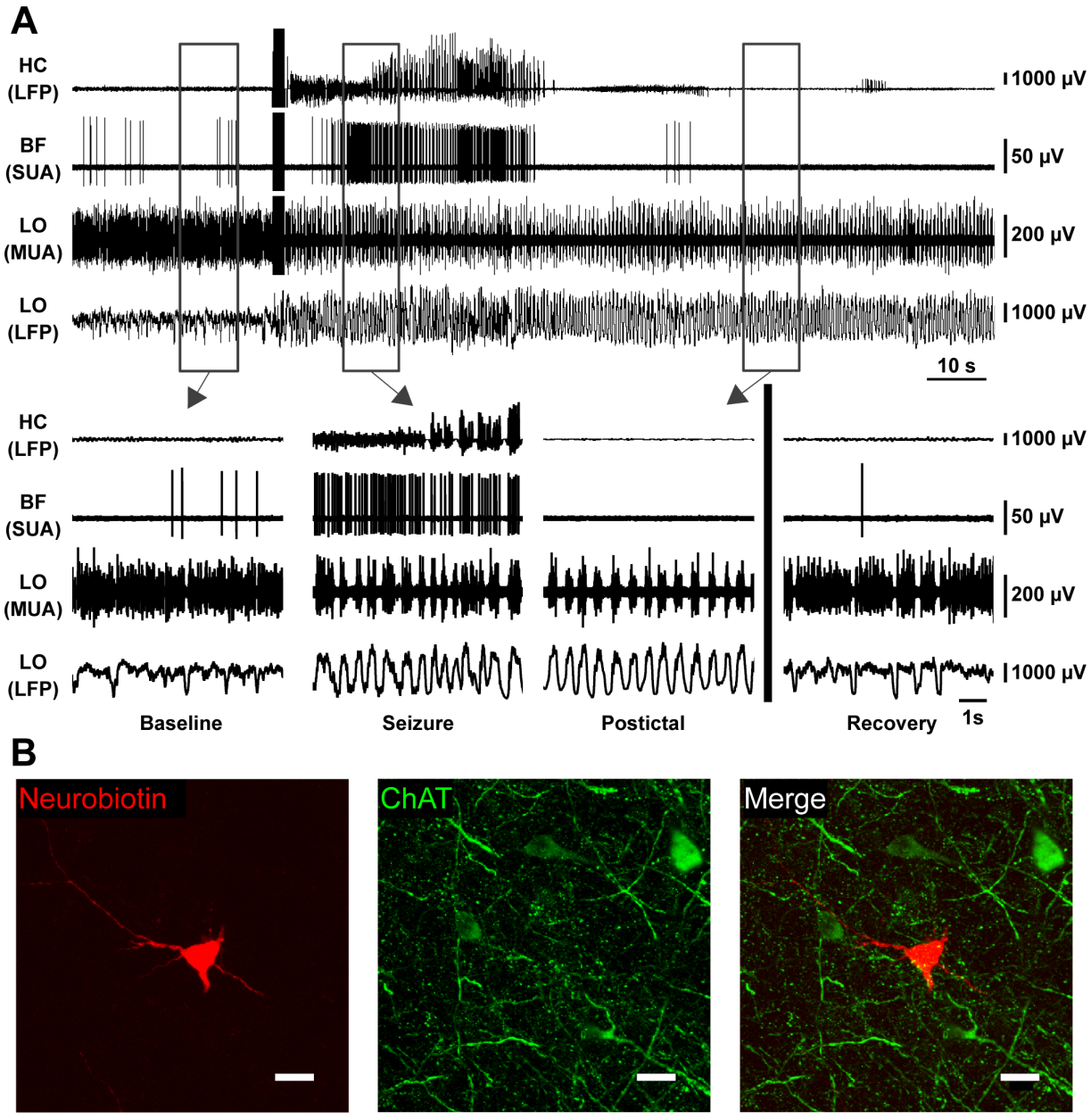
A
HC (LFP)
BF (SUA)
LO (MUA)
LO (LFP)
1000 µV
50 µV
200 µV
1000 µV
10 s
HC (LFP)
BF (SUA)
LO (MUA)
LO (LFP)
1000 µV
50 µV
200 µV
1000 µV
1s
Baseline
Seizure
Postictal
Recovery
B
Neurobiotin
ChAT
Merge

Figure S6, Related to Figure 6

Non-cholinergic neuron in basal forebrain increases firing during seizure activity.

(A) Example of a non-cholinergic neuron during a partial seizure. Expanded segments of baseline, seizure, and postictal recordings from the boxed regions in (A) as well as a recovery period 3 minutes after the stimulus.

(B) Labeled non-cholinergic cell recorded in (A), stained with Neurobiotin in left panel, choline acetyltransferase (ChAT) in middle panel, and merge in right panel. Scale bars are 20 micrometers. HC, hippocampus; BF basal forebrain; LO, lateral orbitofrontal cortex; LFP, local field potential; SUA, single unit (juxtacellular) activity; MUA, multiunit activity.

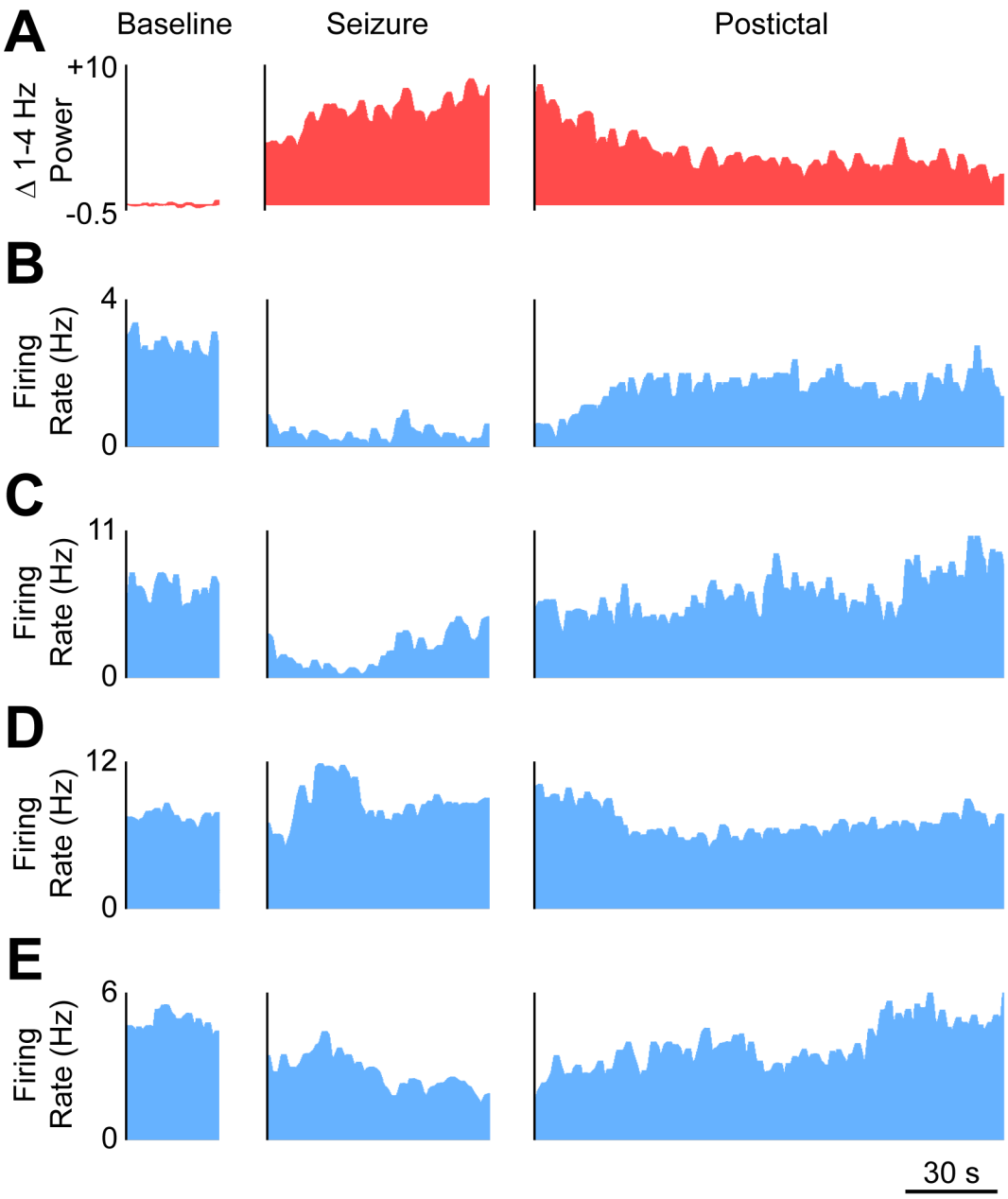
A
Baseline
Seizure
Postictal
Δ 1-4 Hz Power
+10
-0.5
B
Firing Rate (Hz)
4
0
C
Firing Rate (Hz)
11
0
D
Firing Rate (Hz)
12
0
E
Firing Rate (Hz)
6
0
30 s

Figure S7, Related to Figures 4,5, and 6

Juxtaposition of mean firing rates with low-frequency power

(A) Cortical LFP 1-4 Hz power immediately before seizure, during seizure, and immediately following seizure end.

(B-E) Mean firing rates of (B) cholinergic PPT, (C) cholinergic basal forebrain, (D) non-cholinergic PPT, and (E) non-cholinergic basal forebrain.

Left column is data from the 30 seconds prior to seizure initiation. The middle column is whole seizure timecourse scaled to mean seizure duration (54 seizures from 36 animals, mean seizure duration 72.00 seconds ± 4.74 seconds). The right column has postictal data aligned to seizure end without scaling. Histograms are in one-second bins.

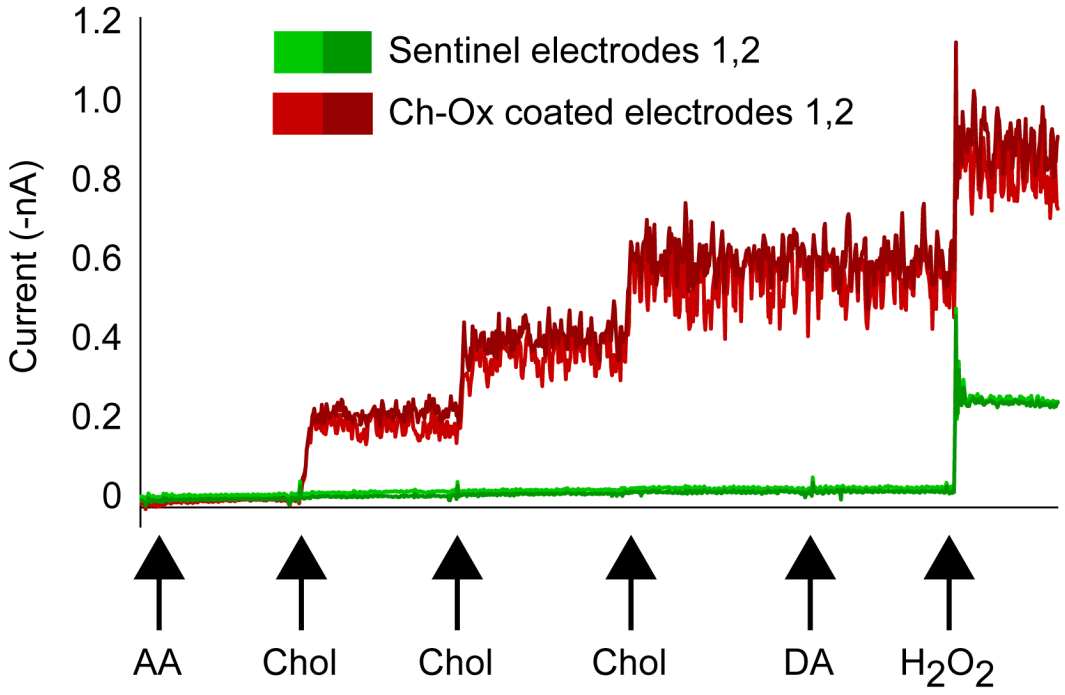
1.2
1.0
0.8
0.6
0.4
0.2
0
Current (-nA)
Sentinel electrodes 1,2
Ch-Ox coated electrodes 1,2
AA
Chol
Chol
Chol
DA
H_2O_2

Figure S8, Related to Figures 7 and 8

Example calibration of choline-sensitive electrode.

Current recordings of *in vitro* calibration. Response to 250 μM addition of ascorbic acid (AA), 20 μM addition of choline (Chol) x 3, 2 μM addition of dopamine (DA) and finally 8.8 μM addition of hydrogen peroxide (H_2O_2). Electrodes are unresponsive to ascorbic acid and dopamine because of the metaphenylenediamine exclusion layer. Only the choline-oxidase coated electrodes are sensitive to choline additions. Finally, all electrodes are sensitive to H_2O_2 indicating that both the choline and sentinel electrodes are functioning normally.

SUPPLEMENTAL EXPERIMENTAL PROCEDURES

Animal preparation and surgery

All procedures were conducted in full compliance with approved institutional animal care and use protocols. A total of 138 adult female Sprague Dawley rats (Charles River Laboratories) weighing 202-365 gram were used in these experiments. 10 animals were used for blood oxygen level-dependent (BOLD) functional magnetic resonance imaging (fMRI) experiments, 108 animals were used for juxtacellular, LFP and MUA experiments, and 20 animals were used for biosensor neurotransmitter recordings.

All surgeries were performed under deep anesthesia with ketamine (90 mg/kg) and xylazine (15 mg/kg). Toe pinch was performed every 15 minutes to determine responsiveness. After surgery animals used in fMRI experiments were allowed at least 6 days of recovery prior to imaging (see below) whereas animals for juxtacellular and neurotransmitter experiments were switched to a low-dose, “light-anesthesia” ketamine (40 mg/kg) and xylazine (7 mg/kg) for immediate recordings as described previously (Englot et al., 2008). All stereotactic coordinates were taken from Paxinos and Watson (Paxinos and Watson, 1998) and were measured in millimeters relative to bregma. Following experiments, animals were sacrificed with Euthasol (Virbac), and brains were harvested for histological analysis and to verify electrode locations.

fMRI experiments

Our implant and imaging methods have been described previously (Englot et al.,

2008). In brief, at least 6 days before fMRI recordings, animals were implanted stereotactically with an MRI-compatible bipolar tungsten electrode (~0.1 MΩ, MicroProbes, WE(35)ST30.1A10) in the right dorsal hippocampus [anteroposterior (AP),-3.8; mediolateral (ML), 2.5; superior–inferior (SI), 2.6]. The electrode was inserted at a 50º angle using a posterior approach in order to allow increased proximity between the rat's head and the MRI coil. The electrode was fixed to the skull with 2-4 nylon screws (MN-0265-015P-C, Small Parts, Inc.) posterior, lateral and anterior to the burr hole using acrylic dental cement. On the day of fMRI recordings, animals were anesthetized with ketamine/xylazine (90/15 mg/kg/hr, I.M.), trachetomized, and artificially ventilated (70% air and 30% O_2). The animal was paralyzed with D-tubocurarine chloride (0.5 mg/kg initial dose, 0.25 mg/kg/2 hour maintenance, I.V.) (Sigma-Aldrich) to prevent movement during imaging and to facilitate artificial breathing. A femoral artery was cannulated (Intramedic PE50 tubing; Becton Dickinson) in order to continuously monitor arterial blood pressure and blood sampling for blood gas and pH (ABL 5 blood gas analyzer, Radiometer Copenhagen). Blood gases, mean arterial blood pressure and pH were maintained within physiological range (Mishra et al., 2011; Schridde et al., 2008). In addition, a femoral vein was cannulated and an IP line was placed (Intramedic PE10 tubing) for the injections of anesthetics, paralyzing agents, and saline. Body temperature was stabilized at 37 º C with a heating pad. To record scalp electroencephalogram (EEG) simultaneously with fMRI, a pair of carbon fiber electrodes (EL254RT, BIOPAC Systems) were placed bilaterally over the cortex between the scalp and the skull. After surgery and preparation for

fMRI experiments, animals were switched to a low-dose ketamine/xylazine (40/7, mg/kg) and maintained under this light anesthesia regimen during seizure induction as described previously (Englot et al., 2008; Englot et al., 2009).

fMRI recordings were acquired on a modified 9.4 T system with Varian (Agilent Technologies, Santa Clara, CA) spectrometer using a custom-built 2 x 1 ^{1}H surface quadrature coil (2.1 cm diameter per coil) for transmitting and receiving radio frequency pulses (Hyde et al., 1987). The magnetic field homogeneity was optimized by localized shimming. High spatial resolution anatomical images were acquired with 10 slices in the coronal plane using gradient-echo or spin-echo contrast. Gradient echo anatomical imaging was obtained using gradient echo multi slice (GEMS) sequence: repetition time (TR), 500 ms; echo time (TE), 4 ms; field-of-view (FOV), 25 x 25 mm; matrix, 256 x 256; in-plane resolution, 98 x 98 μm; contiguous 1 mm slices. Spin echo anatomical imaging was obtained using fast spin echo multi-slice (FSEMS) sequence: TR, 2000 ms; TE, 30 ms; FOV, 25 x 25 mm; matrix, 256 x 256; in-plane resolution, 98 x 98 μm; contiguous 1 mm slices. For fMRI, a single shot spin echo-planar imaging (SE-EPI) sequence was used: TR, 1000 ms; TE, 25 ms; FOV, 25 x 25 mm; matrix, 64 × 64; in-plane resolution, 390 x 390 μm; contiguous slices of 1 mm, with 10 slices obtained in the same planes as anatomical images. The fMRI images were obtained with 1 s acquisition followed by 2 s delay to enable EEG and LFP signals to be readily interpreted during imaging (Englot et al., 2008; Mishra et al., 2011; Schridde et al., 2008). 8 dummy scans were acquired followed by 200 acquisitions (150 acquisitions in one

animal) per 600-second experiment. Partial seizures were induced approximately 1 minute following the beginning of BOLD acquisitions.

Partial seizures were induced approximately 1 minute following the beginning of BOLD acquisitions as described previously (Englot et al., 2008; Englot et al., 2009) with a 2 s stimulus train delivered between the bipolar hippocampal contacts consisting of square wave biphasic (1 ms per phase) pulses at 60 Hz, using an Isolated Pulse Stimulator (model 2100; A-M Systems). The current intensity was titrated by ~200 μA steps to the lowest stimulus intensity (typically 200–800 μA, not exceeding 1000 μA) that would produce a seizure > 30 seconds duration in the hippocampus. EEG signals were filtered (1–300 Hz) using a Data Recording System (model 79D; Grass Instruments). Hippocampal local field potentials (LFPs) from the implanted electrodes were recorded simultaneously with fMRI using two copper connecting wires (custom ~0.3 mm diameter with insulation; Microprobe) bound to the holder with plastic tape and filtered 1–500 Hz (100x gain) with a Microelectrode AC Amplifier (model 1800; A-M Systems). EEG and LFP signals were digitized, recorded (sampling rate, 1000 Hz) using a CEDMicro 1401 and Spike2 software (CED), and processed by applying a low-pass filter at 30 Hz using Spike2 software to reduce residual artifacts in the EEG from magnetic field gradients.

fMRI analysis:

Group t-map: Image analysis was completed using statistical parametric mapping (SPM8, http://www.fil.ion.ucl.ac. uk/spm/) and in-house software written in Matlab

(R2009a, MathWorks, Inc.). BOLD data were masked to remove non-brain pixels and manually co-registered to the animal's own high-resolution anatomical image. Seizure acquisitions were marked by visually analyzing the simultaneously recorded hippocampal LFP. Each acquisition was smoothed using a 2 x 2 voxel Gaussian filter. Baseline was defined by the mean of 10 images just prior to each seizure. For each seizure, mean ictal percent change images were then calculated using all images from the seizure compared to baseline. If an animal had more than one seizure, a mean ictal percent change image was calculated for that animal by taking the mean image across seizures. For group analysis, a registration matrix was computed by manually co-registering high-resolution anatomical images to the anatomical images from a single reference animal and then applying the same registration matrix to the mean ictal percent change matrix for each animal. A 1-sample t-test was then performed on the co-registered percent-change maps using SPM8. A false discovery rate (FDR) corrected *P*-value of 0.05 was used for thresholding.

Time courses: For each animal, regions of interest (ROI) were drawn on its high-resolution anatomical image using a rat-brain atlas(Paxinos and Watson, 1998). Signals were obtained using bilateral ROIs except for in the case of the hippocampus and intralaminar thalamic CL in which only the left side (contralateral to the electrode) was used due to hippocampal electrode imaging artifact in the right ROI (e.g., see **Figures 2** AP slices -3.4 mm and -4.4 mm and **3A**). BOLD signal changes in each ROI were computed as a percent change of the ROI's baseline values. Baseline data included 30 seconds prior to seizure

onset. Seizure data included the entire timecourse of the seizure scaled to mean seizure duration to allow for averaging across animals. Postictal data were aligned to seizure offset without scaling (see **Figure 3B**).

To determine whether the BOLD change was significant during the seizure, a 1-sample two-tailed t-test was computed for each ROI using the mean ROI percent change during the ictal acquisitions. Significance threshold was $P < 0.05$ with Holm-Bonferroni correction.

Acute LFP, MUA, juxtacellular and choline animal preparation

Animals were deeply anesthetized with ketamine/xylazine (90/15 mg/kg). Responsiveness was assessed by toe pinch every 15 minutes. A bipolar electrode (E363/2-2TW, PlasticsOne) for stimulating/recording LFP was stereotactically placed in the left dorsal hippocampus (coordinates above) and affixed to a steel screw (0-80 x 3/32, PlasticsOne) implanted just caudal to the hippocampal burr hole by acrylic dental cement. The two tips of the electrodes were separated by approximately 0.5 mm and approximately 0.5 mm of insulation was shaved off. The electrodes were implanted in the coronal plane. In juxtacellular recordings, a high impedance monopolar electrode (UEWMGGSEDNNM, FHC) for recording local field potential (LFP) and multiunit activity (MUA) was implanted at 20º to the midline into the right lateral orbital frontal cortex (LO) (AP, +4.2; ML, 2.2; SI, 2.4). Additional monopolar electrodes were placed in the lateral septal nuclei (AP, +0.2; ML, +0.5; SI, 5.0) or anterior hypothalamus (AP, -0.4; ML, 0.5; SI, 6.5) as needed. In choline recordings to

avoid shunting amperomety signals via the ground, instead of a high impedance MUA/LFP electrode we used a bipolar LFP electrode for recordings from LO. The LO electrode was prepared in a similar fashion to the hippocampal electrode but implanted in the sagittal plane.

Electrophysiology recordings of MUA and LFP

Collection of extracellular MUA and LFP recordings acquired from monopolar electrodes were described previously (Englot et al., 2008; Englot et al., 2009; Schridde et al., 2008). Briefly, MUA and LFP were acquired using a Microelectrode AC Amplifier (model 1800; A-M Systems) and broadband filtered from 0.1 Hz to 20 kHz (x100 gain). Signals were subsequently filtered using a model 3363 filter (Krohn-Hite) into LFP (0.1 Hz – 100 Hz, x15 gain) and MUA (400 Hz – 10 kHz, x20 gain). LFP from bipolar electrodes was acquired using the same model 1800 amplifier with a broadband filter of 1 Hz – 500 Hz (x1000 gain). Signals were digitized and recorded using a CED Power 1401 and Spike2 software (CED). LFP from monopolar or bipolar electrodes were digitized at 1,000 Hz, MUA from monopolar electrodes were digitized at 20,000 Hz.

MUA and LFP analysis: Recordings were analyzed using in-house software written on Matlab (R2009a, Mathworks, Inc.). Root mean square (RMS) was calculated by squaring the mean signal in 1 second bins and then taking the square root. MUA timecourses were calculated using successive 1 second bins with 0.5 second overlaps. The timecourses are reported as a percent change

from the 30 seconds of baseline prior to seizure initiation (**Figure S1**). We used RMS of the MUA signal as an estimate of action potential firing because this approach has been previously validated in both normal conditions (Logothetis et al., 2001; Shmuel et al., 2006) and during seizures (Englot et al., 2009; Mishra et al., 2011) and template matching may be unreliable during seizures (Schridde et al., 2008). For display purposes, error bars are shown every 9 seconds. To analyze the timecourse of cortical slow wave activity during and following seizures we used a fast Fourier transform (FFT) function in Matlab to obtain 1-4 Hz power in successive 4.096 second bins with 1 second overlap, and again reported results as percent change from the 30 second pre-seizure baseline (**Figure S7A**).

Juxtacellular recordings

Data acquisition: Extracellular single unit recordings were acquired using the juxtacellular method (Pinault, 1996). 1.5 mm glass capillaries (World Precision Instruments, #1B150F-4) were pulled on a Sutter Instruments, P-1000 horizontal puller. The glass electrodes were then bumped under a microscope to produce a flat electrode tip with the desired resistance (15-30 MΩ). The electrodes were filled with 4% Neurobiotin (Vector Laboratories, SP-1120) in saline (0.9% NaCl). The pedunculopontine tegmental nucleus (PPT) was targeted at coordinates (AP, -7.8; ML, 2.0; SI, 7.0) and basal forebrain recordings were targeted at coordinates (AP, 0.7; ML, 2.8; SI, 7) using a micromanipulator (Sutter Instruments, MPC-325). Juxtacellular recordings were acquired on an Axoclamp-

2B amplifier (Molecular Devices, x0.1 gain, current clamp mode, low pass filter < 30 kHz). Single unit activity (SUA) signals were digitized at 20,000 Hz and recorded using a CED Power 1401 and Spike2 software (CED). Seizures were induced as described above for fMRI experiments. Once seizure activity was recorded and the animal returned to baseline, neurons were labeled by passing current pulses (5–200 nA, pulse duration 150 ms, 3 Hz) to drive firing as described previously (Ros et al., 2009). Locations of recovered PPT cells and basal forebrain cells can be found in **Figure S2** and **Figure S5** respectively.

Juxtacellular analysis: Spike sorting on the juxtacellular recordings was performed using Spike2 (CED, v5.20a) and recordings were analyzed using in-house software written on Matlab (R2009a, Mathworks, Inc.). Group firing rate analyses for each group (cholinergic, non-cholinergic, unrecovered) were performed using paired two-tailed t-tests comparing the firing rate for 30 seconds prior to seizure initiation with the firing rate over the course of the seizure. Significance threshold was $P < 0.05$ Holm-Bonferroni corrected. Mean changes in firing rates are graphed and reported ± SEM. For histogram displays (**Figures 6, S4, S7**), firing rates were binned by 1 second with no overlap. “Bursting cells” are those which have >= 1 burst during the recording session. A burst is defined as >= 1 interspike interval <= 10 ms (Ushimaru et al., 2012).

Immunohistochemistry

Tissue preparation: Following juxtacellular recordings, rats were perfused with heparinized saline followed by 4% paraformaldehyde (PFA). Brains were removed and post-fixed for 24-48 hours in PFA. The brainstem was cut at 60 μm sections using a Leica Vibratome (Leica, Inc. VT1000S). Approximately 30 slices were collected and incubated in cyanine 3-conjugated to streptavidin (1:1000; Jackson ImmunoResearch, #016-160-084) diluted in blocking buffer of 5% donkey serum (D9663, Sigma-Aldrich) in PBS-T (0.3% triton-X). Slices were washed for 10 minutes in PBS x 3 and inspected for Neurobiotin filled cells. The slices containing the cell bodies were incubated overnight in goat-α-choline acetyltransferase (Millipore, 1:500, #AB144P) in blocking buffer. After 10 minute washes with PBS-T x 3, the slice was incubated in a secondary antibody for 1 hour (Alexa Fluor 647, donkey α-goat). The slice was washed for 10 minutes in PBS-T x 3, 10 minutes PBS x 1, and mounted for microscopy.

Microscopy: After incubating in cyanine 3-conjugated to streptavidin, slices were "wet mounted" in order to locate the individual slice containing the labeled cell. These cells were visualized on a Zeiss Axiophot microscope with AxioCam HRc and AxioVision software. After slices were identified and stained for ChAT, confocal images were taken on a Zeiss LSM 710 Duo NLO/multiphoton microscope using a C-Apochromat 63x/1.2 W Corr objective. To visualize the cell in the context of the entire slice, additional microscopy was performed on a DM5500 from Leica Microsystems.

Amperometry recordings

Data acquisition: Choline measurements were performed using choline-oxidase enzyme coated amperometric biosensors (Quanteon) on a FAST system (FAST16- mkI, Quanteon). Electrodes were ceramic-based microelectrodes with 4 rectangular (15x333 µm) platinum recording sites in side-by-side pairs (S2, Quanteon). Electrodes were purchased uncoated and prepared with choline oxidase enzyme coating in-house per the manufacturer's instructions. Electrode preparation is described in greater detail elsewhere (Parikh et al., 2004). Briefly, a cross-linked mesh of choline oxidase (Sigma-Aldrich, C5896-100UN), bovine serum albumin (Sigma-Aldrich, A3059-10g), and gluteraldehyde (Sigma-Aldrich, G5882 -10x1ML) was used to coat the bottom two ("coated") electrodes while the upper two ("sentinel") electrodes were coated with the same mixture without choline oxidase. The electrodes were allowed to cure for 3-7 days at 20°C. The day of the experiment, the electrodes were plated with a metaphenylenediamine (*m*-PD) (78450, Sigma-Aldrich) exclusion layer via electropolymerization in order to enhance selectivity for choline over electroactive interferents including ascorbic acid (AA) and dopamine (DA).

After *m*-PD plating, electrodes were calibrated *in vitro* (**Figure S8**) before and after the experiment using fixed potential amperometry. A constant voltage of -0.7 V was applied versus Ag/AgCl reference electrode in a beaker containing 40 ml of 0.05 M PBS. Amperometric currents were digitized at 2 Hz. After a stable baseline was achieved (~30 minutes), aliquots of AA, choline, and DA were added to achieve final concentrations of 250µM AA; 20, 40, and 60 µM choline, and 2 µM (DA). Only electrodes passing the following inclusion criteria were

included: sensitivity for detecting choline on the coated electrodes, > 5 pA/μM; limit of detection (LOD) for choline, < 350 nM; ratio of selectivity for choline and AA, >180:1; linearity of coated electrodes response to increasing analyte concentrations (20-60 μM), Pearson's correlation coefficient (R^2) > 0.99.

Once the electrodes were placed a few hundred μms above the target in the left orbital frontal cortex or thalamic intralaminar CL (AP, -2.5; ML, 1.5; SI, 4.7), the electrodes were lowered slowly to locate "pockets" of fluctuations in choline signal suggesting the presence of local cholinergic terminals in the cortex or thalamus. If the choline signal dramatically increased after lowering, the signal was allowed to return to baseline before seizures were initiated, using the same methods as in fMRI and juxtacellular experiments. At the conclusion of the experiment, animals were deeply anesthetized and toe pinches were administered to activate cholinergic arousal (Mena-Segovia et al., 2008; Zhang et al., 2009). Toe pinches were administered for 1 minute, released for 2 minutes, then administered a second time for 1 minute.

Choline data analysis: In vitro calibration criteria above were used to determine which coated electrodes were used for recordings. Sentinel electrodes were excluded if they malfunctioned during the transfer between *in vitro* beaker calibration and *in vivo* recordings. All signals were first smoothed by subtracting a 10-point moving average. Low-frequency "drift" was removed by subtracting a 400-point moving average. Large artifacts (such as the occasional artifact generated by electrical stimulus to the hippocampus) were removed from the signal to prevent unwanted effects to the drift removal. The first 12.5 seconds of

seizure activity were removed for both display and statistical purposes to remove artifact generated by the 2-second hippocampal stimulus. Statistical analyses were performed for each group (partial seizures and toe pinch) and for each location (cortex and thalamus). The mean choline concentration during 30 seconds of baseline were compared to the mean choline concentration during seizures (after discarding the first 12.5 seconds) or toe pinch (after discarding the first 25 seconds to allow for steady state). A paired two-tailed t-test was performed for each group to determine change from baseline. Holm-Bonferonni correction was used to account for multiple comparisons first for the seizure groups and then separately for the toe pinch groups, with corrected significance threshold $P < 0.05$. Mean changes in concentrations are graphed and reported ± SEM.

Supplemental References

Hyde, J.S., Jesmanowicz, A., Grist, T.M., Froncisz, W., and Kneeland, J.B. (1987). Quadrature detection surface coil. Magnetic resonance in medicine : official journal of the Society of Magnetic Resonance in Medicine / Society of Magnetic Resonance in Medicine 4, 179-184.

Shmuel, A., Augath, M., Oeltermann, A., and Logothetis, N.K. (2006). Negative functional MRI response correlates with decreases in neuronal activity in monkey visual area V1. Nature Neuroscience 9, 569-577.

Zhang, H., Lin, S.C., and Nicolelis, M.A. (2009). Acquiring local field potential information from amperometric neurochemical recordings. J Neurosci Methods 179, 191-200.